Search for an Excess in the Production of Four-Jet Events from e$^+$e$^-$ Collisions at $\sqrt{s} = 130 - 184$ GeV

The OPAL Collaboration

Abstract

Events with four distinct jets from e$^+$e$^-$ collisions, collected by the OPAL detector at centre-of-mass energies between 130 and 184 GeV, are analysed for a peak in the sum of dijet masses. This search is motivated by the ALEPH Collaboration's observation of a clear excess of events with dijet mass sums close to 105 GeV in data taken at centre-of-mass energies of 130 and 136 GeV in 1995. We have observed no significant excess of four-jet events compared to the Standard Model expectation for any dijet mass sum at any energy. Our observation is inconsistent with the excess observed by ALEPH in 1995. Upper limits are determined on the production cross-section as a function of the dijet mass sum.

The OPAL Collaboration

K. Ackerstaff[8], G. Alexander[23], J. Allison[16], N. Altekamp[5], K.J. Anderson[9], S. Anderson[12], S. Arcelli[2], S. Asai[24], S.F. Ashby[1], D. Axen[29], G. Azuelos[18,a], A.H. Ball[17], E. Barberio[8], R.J. Barlow[16], R. Bartoldus[3], J.R. Batley[5], S. Baumann[3], J. Bechtluft[14], T. Behnke[8], K.W. Bell[20], G. Bella[23], S. Bentvelsen[8], S. Bethke[14], S. Betts[15], O. Biebel[14], A. Biguzzi[5], S.D. Bird[16], V. Blobel[27], I.J. Bloodworth[1], M. Bobinski[10], P. Bock[11], D. Bonacorsi[2], M. Boutemeur[34], S. Braibant[8], L. Brigliadori[2], R.M. Brown[20], H.J. Burckhart[8], C. Burgard[8], R. Bürgin[10], P. Capiluppi[2], R.K. Carnegie[6], A.A. Carter[13], J.R. Carter[5], C.Y. Chang[17], D.G. Charlton[1,b], D. Chrisman[4], P.E.L. Clarke[15], I. Cohen[23], J.E. Conboy[15], O.C. Cooke[8], C. Couyoumtzelis[13], R.L. Coxe[9], M. Cuffiani[2], S. Dado[22], C. Dallapiccola[17], G.M. Dallavalle[2], R. Davis[30], S. De Jong[12], L.A. del Pozo[4], A. de Roeck[8], K. Desch[8], B. Dienes[33,d], M.S. Dixit[7], M. Doucet[18], E. Duchovni[26], G. Duckeck[34], I.P. Duerdoth[16], D. Eatough[16], P.G. Estabrooks[6], E. Etzion[23], H.G. Evans[9], M. Evans[13], F. Fabbri[2], A. Fanfani[2], M. Fanti[2], A.A. Faust[30], L. Feld[8], F. Fiedler[27], M. Fierro[2], H.M. Fischer[3], I. Fleck[8], R. Folman[26], D.G. Fong[17], M. Foucher[17], A. Fürtjes[8], D.I. Futyan[16], P. Gagnon[7], J.W. Gary[4], J. Gascon[18], S.M. Gascon-Shotkin[17], N.I. Geddes[20], C. Geich-Gimbel[3], T. Geralis[20], G. Giacomelli[2], P. Giacomelli[4], R. Giacomelli[2], V. Gibson[5], W.R. Gibson[13], D.M. Gingrich[30,a], D. Glenzinski[9], J. Goldberg[22], M.J. Goodrick[5], W. Gorn[4], C. Grandi[2], E. Gross[26], J. Grunhaus[23], M. Gruwé[27], C. Hajdu[32], G.G. Hanson[12], M. Hansroul[8], M. Hapke[13], C.K. Hargrove[7], P.A. Hart[9], C. Hartmann[3], M. Hauschild[8], C.M. Hawkes[5], R. Hawkings[27], R.J. Hemingway[6], M. Herndon[17], G. Herten[10], R.D. Heuer[8], M.D. Hildreth[8], J.C. Hill[5], S.J. Hillier[1], P.R. Hobson[25], A. Hocker[9], R.J. Homer[1], A.K. Honma[28,a], D. Horváth[32,c], K.R. Hossain[30], R. Howard[29], P. Hüntemeyer[27], D.E. Hutchcroft[5], P. Igo-Kemenes[11], D.C. Imrie[25], K. Ishii[24], A. Jawahery[17], P.W. Jeffreys[20], H. Jeremie[18], M. Jimack[1], A. Joly[18], C.R. Jones[5], M. Jones[6], U. Jost[11], P. Jovanovic[1], T.R. Junk[8], J. Kanzaki[24], D. Karlen[6], V. Kartvelishvili[16], K. Kawagoe[24], T. Kawamoto[24], P.I. Kayal[30], R.K. Keeler[28], R.G. Kellogg[17], B.W. Kennedy[20], J. Kirk[29], A. Klier[26], S. Kluth[8], T. Kobayashi[24], M. Kobel[10], D.S. Koetke[6], T.P. Kokott[3], M. Kolrep[10], S. Komamiya[24], R.V. Kowalewski[28], T. Kress[11], P. Krieger[6], J. von Krogh[11], P. Kyberd[13], G.D. Lafferty[16], R. Lahmann[17], W.P. Lai[19], D. Lanske[14], J. Lauber[15], S.R. Lautenschlager[31], I. Lawson[28], J.G. Layter[4], D. Lazic[22], A.M. Lee[31], E. Lefebvre[18], D. Lellouch[26], J. Letts[12], L. Levinson[26], B. List[8], S.L. Lloyd[13], F.K. Loebinger[16], G.D. Long[28], M.J. Losty[7], J. Ludwig[10], D. Lui[12], A. Macchiolo[2], A. Macpherson[30], M. Mannelli[8], S. Marcellini[2], C. Markopoulos[13], C. Markus[3], A.J. Martin[13], J.P. Martin[18], G. Martinez[17], T. Mashimo[24], P. Mättig[26], W.J. McDonald[30], J. McKenna[29], E.A. Mckigney[15], T.J. McMahon[1], R.A. McPherson[28], F. Meijers[8], S. Menke[3], F.S. Merritt[9], H. Mes[7], J. Meyer[27], A. Michelini[2], S. Mihara[24], G. Mikenberg[26], D.J. Miller[15], A. Mincer[22,e], R. Mir[26], W. Mohr[10], A. Montanari[2], T. Mori[24], S. Mihara[24], K. Nagai[26], I. Nakamura[24], H.A. Neal[12], B. Nellen[3], R. Nisius[8], S.W. O'Neale[1], F.G. Oakham[7], F. Odorici[2], H.O. Ogren[12], A. Oh[27], N.J. Oldershaw[16], M.J. Oreglia[9], S. Orito[24], J. Pálinkás[33,d], G. Pásztor[32], J.R. Pater[16], G.N. Patrick[20], J. Patt[10], R. Perez-Ochoa[8], S. Petzold[27], P. Pfeifenschneider[14], J.E. Pilcher[9], J. Pinfold[30], D.E. Plane[8], P. Poffenberger[28], B. Poli[2], A. Posthaus[3], C. Rembser[8], S. Robertson[28], S.A. Robins[22], N. Rodning[30], J.M. Roney[28], A. Rooke[15], A.M. Rossi[2], P. Routenburg[30], Y. Rozen[22], K. Runge[10], O. Runolfsson[8], U. Ruppel[14], D.R. Rust[12], K. Sachs[10], T. Saeki[24], O. Sahr[34], W.M. Sang[25], E.K.G. Sarkisyan[23], C. Sbarra[29], A.D. Schaile[34], O. Schaile[34], F. Scharf[3], P. Scharff-Hansen[8], J. Schieck[11],

P. Schleper[11], B. Schmitt[8], S. Schmitt[11], A. Schöning[8], M. Schröder[8], M. Schumacher[3],
C. Schwick[8], W.G. Scott[20], T.G. Shears[8], B.C. Shen[4], C.H. Shepherd-Themistocleous[8],
P. Sherwood[15], G.P. Siroli[2], A. Sittler[27], A. Skillman[15], A. Skuja[17], A.M. Smith[8], G.A. Snow[17],
R. Sobie[28], S. Söldner-Rembold[10], R.W. Springer[30], M. Sproston[20], K. Stephens[16], J. Steuerer[27],
B. Stockhausen[3], K. Stoll[10], D. Strom[19], R. Ströhmer[34], P. Szymanski[20], R. Tafirout[18],
S.D. Talbot[1], P. Taras[18], S. Tarem[22], R. Teuscher[8], M. Thiergen[10], M.A. Thomson[8], E. von
Törne[3], E. Torrence[8], S. Towers[6], I. Trigger[18], Z. Trócsányi[33], E. Tsur[23], A.S. Turcot[9],
M.F. Turner-Watson[8], I. Ueda[24], P. Utzat[11], R. Van Kooten[12], P. Vannerem[10], M. Verzocchi[10],
P. Vikas[18], E.H. Vokurka[16], H. Voss[3], F. Wäckerle[10], A. Wagner[27], C.P. Ward[5], D.R. Ward[5],
P.M. Watkins[1], A.T. Watson[1], N.K. Watson[1], P.S. Wells[8], N. Wermes[3], J.S. White[28],
G.W. Wilson[27], J.A. Wilson[1], T.R. Wyatt[16], S. Yamashita[24], G. Yekutieli[26], V. Zacek[18],
D. Zer-Zion[8]

[1]School of Physics and Astronomy, University of Birmingham, Birmingham B15 2TT, UK
[2]Dipartimento di Fisica dell' Università di Bologna and INFN, I-40126 Bologna, Italy
[3]Physikalisches Institut, Universität Bonn, D-53115 Bonn, Germany
[4]Department of Physics, University of California, Riverside CA 92521, USA
[5]Cavendish Laboratory, Cambridge CB3 0HE, UK
[6]Ottawa-Carleton Institute for Physics, Department of Physics, Carleton University, Ottawa, Ontario K1S 5B6, Canada
[7]Centre for Research in Particle Physics, Carleton University, Ottawa, Ontario K1S 5B6, Canada
[8]CERN, European Organisation for Particle Physics, CH-1211 Geneva 23, Switzerland
[9]Enrico Fermi Institute and Department of Physics, University of Chicago, Chicago IL 60637, USA
[10]Fakultät für Physik, Albert Ludwigs Universität, D-79104 Freiburg, Germany
[11]Physikalisches Institut, Universität Heidelberg, D-69120 Heidelberg, Germany
[12]Indiana University, Department of Physics, Swain Hall West 117, Bloomington IN 47405, USA
[13]Queen Mary and Westfield College, University of London, London E1 4NS, UK
[14]Technische Hochschule Aachen, III Physikalisches Institut, Sommerfeldstrasse 26-28, D-52056 Aachen, Germany
[15]University College London, London WC1E 6BT, UK
[16]Department of Physics, Schuster Laboratory, The University, Manchester M13 9PL, UK
[17]Department of Physics, University of Maryland, College Park, MD 20742, USA
[18]Laboratoire de Physique Nucléaire, Université de Montréal, Montréal, Quebec H3C 3J7, Canada
[19]University of Oregon, Department of Physics, Eugene OR 97403, USA
[20]Rutherford Appleton Laboratory, Chilton, Didcot, Oxfordshire OX11 0QX, UK
[22]Department of Physics, Technion-Israel Institute of Technology, Haifa 32000, Israel
[23]Department of Physics and Astronomy, Tel Aviv University, Tel Aviv 69978, Israel
[24]International Centre for Elementary Particle Physics and Department of Physics, University of Tokyo, Tokyo 113, and Kobe University, Kobe 657, Japan
[25]Institute of Physical and Environmental Sciences, Brunel University, Uxbridge, Middlesex UB8 3PH, UK

[26]Particle Physics Department, Weizmann Institute of Science, Rehovot 76100, Israel

[27]Universität Hamburg/DESY, II Institut für Experimental Physik, Notkestrasse 85, D-22607 Hamburg, Germany

[28]University of Victoria, Department of Physics, P O Box 3055, Victoria BC V8W 3P6, Canada

[29]University of British Columbia, Department of Physics, Vancouver BC V6T 1Z1, Canada

[30]University of Alberta, Department of Physics, Edmonton AB T6G 2J1, Canada

[31]Duke University, Dept of Physics, Durham, NC 27708-0305, USA

[32]Research Institute for Particle and Nuclear Physics, H-1525 Budapest, P O Box 49, Hungary

[33]Institute of Nuclear Research, H-4001 Debrecen, P O Box 51, Hungary

[34]Ludwigs-Maximilians-Universität München, Sektion Physik, Am Coulombwall 1, D-85748 Garching, Germany

[a] and at TRIUMF, Vancouver, Canada V6T 2A3

[b] and Royal Society University Research Fellow

[c] and Institute of Nuclear Research, Debrecen, Hungary

[d] and Department of Experimental Physics, Lajos Kossuth University, Debrecen, Hungary

1   Introduction

In a run of LEP in 1995 at centre-of-mass energies of $\sqrt{s} = 130$ and 136 GeV, the ALEPH Collaboration observed [1] an excess of events with four distinct jets compared with the Standard Model expectation. Such an excess could be due to the production of new particles X and Y, each decaying into two hadronic jets in the process $e^+e^- \to XY \to$ four jets. The two particles could have equal or unequal masses. Grouping the jets into pairs, calculating their pair invariant masses M_{ij} and M_{kl}, and selecting the combination yielding the smallest mass difference $\Delta M = |M_{ij} - M_{kl}|$, ALEPH observed a clustering of nine events in a mass window 6.3 GeV wide centred around $M = M_{ij} + M_{kl} \approx 105$ GeV, with a Standard Model expectation of 0.8 events in this mass window. The choice of the combination with the minimum ΔM would tend to favour the selection of particles of equal mass or with a small mass difference.

In response to this observation, the OPAL Collaboration performed an analysis that closely followed the selection of Reference [1]. In its 130 and 136 GeV data from 1995, OPAL observed seven events with M between 60 and 130 GeV, with an expected Standard Model background of 6.4±0.6 events. In the signal region indicated by ALEPH, OPAL observed one event, consistent with the expected Standard Model background of 0.8 ± 0.2 events [2]. The estimated efficiency of the OPAL analysis and the resolution on the dijet mass sum are similar to those obtained by ALEPH. Consequently, the OPAL detector would be expected to have a sensitivity comparable to the ALEPH detector for a four-jet signal should one exist. The ALEPH Collaboration also reported a slight excess at the higher centre-of-mass energies of 161 and 172 GeV [3]. The DELPHI Collaboration observed no significant peak at 105 GeV in a similar analysis using their 1995 data at 130 and 136 GeV [4]. The L3 Collaboration likewise reported no excess of events in the indicated mass window for $\sqrt{s} = 130$–172 GeV [5]. Nonetheless, there has been a great deal of theoretical speculation on the cause of the excess observed by ALEPH [6, 7, 8].

In 1997, LEP made short runs at $\sqrt{s} = 130$ and 136 GeV with an integrated luminosity similar to that of 1995 at these centre-of-mass energies to test again the signal hypothesis. We add these data to our sample described in Reference [2], and also include data collected at 161, 172 and 183 GeV. To search for the class of events observed by ALEPH in a model independent fashion, we have performed analyses on the OPAL data as close as possible to the ALEPH analyses at these energies [3]. However, above the kinematic threshold for W-pair production, a veto is imposed to suppress this new source of background and results are presented with and without this requirement.

The comparison of results of the OPAL emulation of the ALEPH selection to the ALEPH observation of an excess does not depend upon the underlying model of possible new physics if only the number of observed events is compared. In the context of a model of the process $e^+e^- \to XY \to$ four jets, a separate analysis is also presented that is intended to improve the sensitivity for values up to 30 GeV of the difference in mass between the two produced particles. This broader search is motivated by the fact that an analysis performed by the ALEPH Collaboration, using a kinematic fit which constrains the masses of the two dijet systems to be equal [9], indicates that the excess events are not consistent with the hypothesis that the produced particles have equal mass. Furthermore, compared with the ALEPH emulation analysis, this OPAL-specific analysis is estimated to be more sensitive to a four-jet signal of equal-mass

particle production at higher energies, and its efficiency is less dependent on the flavour of the final-state quarks. It is used in addition to the emulation of the ALEPH analysis to set cross-section limits as function of the dijet mass sum, and also to provide limits in the case of nonzero mass difference.

2   The OPAL Detector

A detailed description of the OPAL detector can be found elsewhere [10]. OPAL's nearly complete solid angle coverage and excellent hermeticity enable it to detect the four-jet final state with high efficiency. The central tracking detector consists of a two-layer silicon microstrip detector [11] with polar angle[1] coverage $|\cos\theta| < 0.9$, immediately surrounding the beam-pipe, followed by a high-precision vertex drift chamber, a large-volume jet chamber and z-chambers, all in a uniform 0.435 T axial magnetic field. A lead-glass electromagnetic calorimeter is located outside the magnet coil, which, in combination with the forward calorimeter, gamma catcher and silicon-tungsten luminometer [12], complete the geometrical acceptance down to 24 mrad from the beam direction. The silicon-tungsten luminometer serves to measure the integrated luminosity using small-angle Bhabha scattering events [13]. The magnet return yoke is instrumented with streamer tubes for hadron calorimetry and is surrounded by several layers of muon chambers.

3   Data and Monte Carlo simulations

The data used in these analyses were collected in five separate running periods. The energies [14] and integrated luminosities [13] for the five data samples are given in Table 1. The 130 and 136 GeV data of 1995 and 1997 are collectively referred to in this letter as the 133 GeV data. The other three samples are referred to as the 161 GeV data, the 172 GeV data, and the 183 GeV data, and are analysed separately.

The main backgrounds for the selection of anomalous four-jet events are $Z^0/\gamma^* \to q\bar{q}$ production and Standard Model four-fermion production processes. Monte Carlo samples modelling the backgrounds have been prepared using PYTHIA 5.7 [15] for the $Z^0/\gamma^* \to q\bar{q}$ process and EXCALIBUR [16] and grc4f [17] for the Standard Model four-fermion processes, all using JETSET 7.4's parton shower and hadronization models [15]. For the generation of Standard Model four-fermion processes, the W mass is taken to be 80.33 GeV. Two-photon processes generated by PYTHIA, HERWIG [18], and PHOJET [19] were used to estimate the contribution of these processes to the Standard Model background in the early stages of the analysis.

The signal detection efficiencies were estimated using the HZHA generator [20] to simulate the production of supersymmetric Higgs bosons $e^+e^- \to h^0A^0 \to b\bar{b}b\bar{b}$ as a model for the

---

[1]OPAL uses a right-handed coordinate system where the $+z$ direction is along the electron beam and where $+x$ points to the centre of the LEP ring. The polar angle, θ, is defined with respect to the $+z$ direction and the azimuthal angle, ϕ, with respect to the $+x$ direction.

$\sqrt{s}$ (GeV)	Year	$\int \mathcal{L}\mathrm{d}t$ (pb^{-1})
130.3	1995	2.7
136.2	1995	2.6
130.0	1997	2.6
136.0	1997	3.4
161.3	1996	10.0
172.1	1996	10.3
182.7	1997	57.1

Table 1: *Summary of the data samples, luminosity-weighted centre-of-mass energies, year of collection, and integrated luminosities used in these analyses.*

signal process $\mathrm{e^+e^-} \to \mathrm{XY} \to 4$ jets. Samples with decays into other quark flavours were also used to check for flavour dependence. All Monte Carlo samples were processed through a full simulation of the OPAL detector [21].

4   Analysis and Results

The main features of the signal process are four well-defined, energetic, hadronic jets and a total visible event energy close to the centre-of-mass energy. The Standard Model background expectation changes considerably in size and composition between $\sqrt{s} =$133 GeV and 183 GeV. At 133 GeV, the main background comes from $\mathrm{Z^0}/\gamma^* \to \mathrm{q\bar{q}}$ both with or without initial-state radiation and accompanied by hard gluon emission. Above the threshold for $\mathrm{e^+e^-} \to \mathrm{W^+W^-}$ at $\sqrt{s} = 161$ GeV, the background from Standard Model four-fermion processes is important and becomes larger with increasing $\sqrt{s}$. A procedure to reject $\mathrm{W^+W^-} \to \mathrm{q\bar{q}q\bar{q}}$ is implemented for centre-of-mass energies of 161 GeV and above.

Events are reconstructed from charged particle tracks and energy deposits ("clusters") in the electromagnetic and hadronic calorimeters. Tracks are required to originate from close to the interaction point, to have more than a minimum number of hits in the jet chamber, and to have a transverse momentum greater than 0.1 GeV and a total momentum less than 100 GeV [22]. Energy clusters in the electromagnetic and hadron calorimeters are required to exceed minimum energy thresholds. Tracks and clusters passing these quality requirements are then processed to reduce double-counting of energy and momentum in the event by matching charged tracks with calorimeter clusters. The energy-momentum flow obtained with this algorithm [23] is used throughout the analysis. Energy measured in the forward detectors, covering $|\cos\theta| > 0.985$, has not been included in the analyses presented here.

Selection criteria emulating the ALEPH analysis [1] will first be described followed by the description of another set of requirements for event selection in an OPAL-specific analysis. Efficiencies and backgrounds for the two analyses are given followed by estimates of systematic errors on these quantities.

4.1 OPAL Emulation of the ALEPH Selection

The procedure for selecting four-jet hadronic events and reconstructing the dijet masses is described below, emulating the ALEPH selection as described in Reference [1] and subsequent modifications and developments as described in Reference [3]. The number of events retained after each cut in sequence is given in Table 2, together with the expectation from $Z^0/\gamma^* \to q\bar{q}$, Standard Model four-fermion and two-photon background processes, for $\sqrt{s} = 133$ GeV and for the sum over all centre-of-mass energies. Table 2 also lists the efficiencies for the reference $h^0 A^0$ Monte Carlo at $\sqrt{s} = 133$ GeV after each step.

1. Events are required to have at least five charged tracks and seven electromagnetic calorimeter clusters. The sum of the electromagnetic calorimeter cluster energies should be at least 10% of the centre-of-mass energy, and the electromagnetic calorimeter energy is required to be roughly balanced along the beam direction: $\sum E_i \cos\theta_i \leq 0.65 \sum E_i$, where the sums run over measured electromagnetic calorimeter clusters. The properties of this selection are detailed in Reference [22].

2. To remove events with a real Z^0 and large initial-state radiation (radiative return events), events must satisfy $|p_z^{\mathrm{vis}}| \leq K(M_{\mathrm{vis}} - 90 \text{ (GeV)})$, where p_z^{vis} is the momentum sum along the beam direction and $M_{\mathrm{vis}} = \sqrt{E_{\mathrm{vis}}^2 - p_{\mathrm{vis}}^2}$ is the total observed mass. K is a coefficient depending on $\sqrt{s}$. For the 133 GeV sample, $K = 0.75$; for the 161 GeV sample, $K = 1.50$; and for the 172 GeV and 183 GeV samples, $K = 1.65$.

3. Jets are formed with the Durham jet-finding algorithm [24] with its resolution parameter y_{cut} set to 0.008. Selected events are required to have four or more jets. For events with five or more jets, the jet pair with the smallest invariant mass is combined into a single jet and this procedure is repeated until four jets are left.

4. The contribution of radiative return events is further reduced by requiring for each jet that the energy observed in the electromagnetic calorimeter, after subtracting the energy expected to have been deposited by the jet's charged hadrons, is less than 80% of the jet energy. The expected hadronic energy in the electromagnetic calorimeter is calculated using a track-cluster matching algorithm [23].

5. All jet masses are required to exceed 1.0 GeV to suppress further the contribution from radiative return events.

6. The energies and momenta of each jet are rescaled imposing conservation of energy and momentum for the event using the beam energy constraint. The jet velocities $\vec{\beta}_i = \vec{p}_i/E_i$ are held fixed in the scaling. If one or more scaling factors is negative, the event is rejected. The rescaled jet energies and momenta are used in the following stages of the selection.

7. To suppress events involving gluon radiation, all two-jet combinations are required to have an invariant mass of more than 19.2% of the centre-of-mass energy. This initially corresponded to 25 GeV for the 133 GeV sample.

8. All combinations of jet pairs must have a sum of the individual jet masses $(M_i + M_j) > 10$ GeV.

9. All combinations of jet pairs must have a total charged multiplicity of at least 10.

10. W-pair veto: For the 161 GeV data sample, a requirement is placed on the dijet mass sum for each of the three possible pairings of jets: $M \leq 150$ GeV for the pairing with the smallest ΔM, $M \leq 152$ GeV for the pairing with intermediate ΔM, and $M \leq 156$ GeV for the pairing with the largest ΔM. For the 172 and 183 GeV data, it is required that $|M - 160| \geq 10$ GeV for the pairing with the smallest mass difference if ΔM is less than 15 GeV, and the same condition is applied to the pairing with the second-smallest mass difference if the second smallest ΔM is less than 30 GeV. No W-pair veto is applied to the 133 GeV sample.

Cut	(1)	(2)	(3)	(4)	(5)	(6)	(7)	(8)	(9)	(10)
$\sqrt{s} = 133$ GeV										
$Z^0/\gamma^* \to q\bar{q}$	3151.	1185.	153.2	55.1	50.8	45.7	22.5	18.0	14.6	14.6
4-Fermion	24.5	16.1	4.2	3.6	3.1	3.0	1.6	1.1	0.7	0.7
$\gamma\gamma$	161.0	8.9	1.7	1.7	1.7	1.7	1.1	0.0	0.0	0.0
Total SM backg.	3337.	1211.	159.2	60.4	55.6	50.4	25.2	19.1	15.3	15.3
Observed	3372	1165	147	51	47	42	19	16	13	13
Sig. effic., ϵ_{hA} (%)	99.8	90.2	69.0	68.6	67.4	67.2	65.4	48.6	45.4	45.4
All $\sqrt{s}$ 130–184 GeV										
$Z^0/\gamma^* \to q\bar{q}$	10456.	4450.	481.1	188.7	176.7	155.0	68.2	59.7	49.2	40.2
4-Fermion	1098.	913.0	476.0	428.0	400.5	364.8	258.1	236.3	191.7	74.2
$\gamma\gamma$	450.7	26.3	2.7	2.2	2.1	1.8	1.0	0.0	0.0	0.0
Total SM backg.	12004.	5389.	959.9	618.9	579.4	521.6	327.4	295.9	240.8	114.3
Observed	12617	5461	984	635	592	527	328	299	240	92

Table 2: *Event counts observed by OPAL at the various selection stages, with backgrounds estimated using PYTHIA for $Z^0/\gamma^* \to q\bar{q}$, EXCALIBUR and grc4f for Standard Model four-fermion processes, and PYTHIA and PHOJET for two-photon processes. Signal efficiencies at 133 GeV for $h^0 A^0$ (see text) for $M_{h^0} = M_{A^0} = 55$ GeV are also listed.*

The dijet mass sum for the combination with the smallest dijet mass difference is shown in Figure 1, separately for the data samples at the four different values of $\sqrt{s}$, after the W-pair veto. The expected Standard Model background distribution is shown with the data for each case. No significant excess is observed at any of the centre-of-mass energies.

The sensitivity of the analysis to a peak at a particular dijet mass sum depends on the resolution and may be affected by energy scale biases. The resolution was investigated using the HZHA event generator [20] to model the process $e^+e^- \to h^0 A^0$. The masses of both the h^0 and the A^0 are taken to be equal to 55 GeV with negligible width. The resolutions found for the reconstructed dijet mass sum M for the combination with the smallest ΔM are $\sigma_M = 2.0$, 2.8, 3.0, and 3.0 GeV for $\sqrt{s} = 133$ GeV, 161 GeV, 172 GeV, and 183 GeV, respectively. These resolutions do not include effects of significant non-Gaussian tails which arise from wrong jet-pair combinations, where the correct jet-pair combination is when each of the two jets comes

8

from the decay of the same particle. For example, at $\sqrt{s} = 133$ GeV, 38% of the events fall into these tails. This definition of the resolution and tails is the same as that used in the ALEPH publication [1] and the resolution values found are similar to those of ALEPH. The degradation of mass resolution with increasing energy arises from the scaling of the jet energies to the beam energy and also from the energy dependence of the detector resolution.

Studies of the $h^0 A^0$ signal Monte Carlo with samples generated with input masses adding to 110 GeV at each centre-of-mass energy show that the reconstructed M distributions have peaks at masses consistent with this input value within their errors of approximately 0.5 GeV. Studies of events from radiative returns to the Z^0, $q\bar{q}\gamma$, were also used to check that the Z^0 peak is well simulated in position and shape, further indicating that there is no significant bias in M or degradation in resolution inherent to the selection or the mass reconstruction procedure.

For the 133 GeV signal Monte Carlo, if the reconstructed dijet mass sum for the jet-pair combination having the smallest ΔM is required to be within $2\sigma_M$ (4.0 GeV) of the generated mass sum, the efficiency obtained is 26.6%, which is 60% of the efficiency obtained without the requirement on M. The efficiencies and expected backgrounds both before and after the mass window cut are similar to those obtained by ALEPH [1] so that for the same integrated luminosity, the observed number of events can be directly compared to the number observed in Reference [1]. At higher centre-of-mass energies, accepting events only in a mass window of width $\pm 2\sigma_M$ results in efficiencies of 18–21% which is 66–69% of the efficiency before the mass window requirement.

To search for an excess of four-jet events with dijet mass sums near 105 GeV as motivated by Reference [1], events satisfying $|M - 105 \text{ GeV}| < 2\sigma_M$ for the combination with the smallest ΔM were counted and the Standard Model backgrounds were estimated. These mass windows are shown in Figure 1 and the results of the searches within these mass regions are given in Table 3 both before and after the W-pair veto, when applicable. No significant excess is seen in any sample. Combining data from all centre-of-mass energies, nine events are observed while 11.5 ± 0.4 are expected from Standard Model processes.

Data Sample	Without W-Pair Veto			With W-Pair Veto		
	Observed	Expected	Sig. eff., ϵ_{hA}	Observed	Expected	Sig. eff., ϵ_{hA}
133 GeV	1	1.7 ± 0.2	26.6%	1	1.7 ± 0.2	26.6%
161 GeV	1	1.5 ± 0.1	26.2%	0	1.0 ± 0.1	18.4%
172 GeV	3	2.9 ± 0.1	28.3%	0	1.8 ± 0.1	20.7%
183 GeV	13	11.5 ± 0.4	26.0%	8	7.0 ± 0.3	18.3%
Total	18	17.7 ± 0.5	—	9	11.5 ± 0.4	—

Table 3: *Observed event count and expected Standard Model background for selected events close to 105 GeV, for the combination with the smallest ΔM, before and after the W-pair veto. No W-pair veto is applied for the 133 GeV data. The mass window is chosen to allow events that are within $\pm 2\sigma_M$ of 105 GeV to be included, where σ_M is the expected experimental resolution on M as given in the text. Signal efficiencies apply to $h^0 A^0$ production with $M_{h^0} = M_{A^0} = 55$ GeV.*

Figure 2 shows the distribution of the dijet mass sum for the jet pairing with the smallest ΔM for all running periods combined, with and without the W-pair veto. The data agree well with the Standard Model background simulation and no excess is observed in the region $99.0 < M < 111.0$ GeV, where the width has been chosen to accommodate the resolution at the highest energy. A clear peak may be seen at twice the W mass in the sample before the W-pair veto.

To test for a peak in the dijet mass sum distribution for arbitrary mass M and independent of histogram binning, the positions of the mass windows were scanned over the full range of M. The results are shown in Figure 2(c) for the combined data samples. The figure displays the event counts within windows of fixed width but whose centres are adjusted in steps of 50 MeV. The width of the mass window is ± 4.0, ± 5.6, ± 6.0 GeV, and ± 6.0 GeV for the 133, 161, 172, and 183 GeV data samples, respectively, to reflect the resolution. The contents of nearby bins in these scans have high statistical correlations. No significant excess is observed in the mass window scan at any value of the dijet mass sum. In particular, no choice of binning produces a peak near 105 GeV.

To check for a possible signal in the fraction of events with wrong jet-pair combinations, the dijet mass sum for the jet pairing with the second-smallest ΔM was also considered. If the mass difference of a pair of objects produced together were 20 GeV, the correct jet pairing would yield the smallest ΔM for roughly half of the signal, and the second-smallest ΔM for most of the remainder. In the ALEPH analysis [1], including the second combination to the dijet mass sum distribution resulted in three additional events within the mass window with an additional 1.2 events expected from Standard Model processes. Figure 3 shows the effect of adding the dijet mass sum distributions for the smallest and second-smallest ΔM combinations for different centre-of-mass energies. The distributions agree well with the Standard Model prediction and no peak arises when the second combination is included.

4.2 OPAL-Specific Analysis

In the above analysis, an emulation of the ALEPH selection criteria was applied to the OPAL data to test for the presence of events of the type observed by ALEPH. The selection described below is an OPAL-specific analysis in which the sensitivity has been maximised for detecting a possible signal for the process $e^+e^- \rightarrow XY$ in the form of an excess of events with similar mass sums $M = M_X + M_Y$ in the four-jet topology. The analysis is designed to retain sensitivity even when the mass difference $\Delta M = |M_X - M_Y|$ is as large as 30 GeV. Efficiencies and backgrounds are estimated for different values of M and ΔM.

The cuts are designed to be as insensitive as possible to the flavours of the final state quarks. Although the methods employed at each of the centre-of-mass energies are similar, the optimal cut values in most cases depend on $\sqrt{s}$.

1. The events must pass the hadronic final state requirement of cut 1 in Section 4.1.

2. The effective centre-of-mass energy after initial-state radiation, $\sqrt{s'}$, calculated using the method described in Reference [26], has to be at least $0.87\sqrt{s}$. The measured visible mass,

M_{vis}, is required to be between $\sqrt{s}-40$ GeV and $\sqrt{s}+30$ GeV at 133 GeV, between 100 and 200 GeV at $\sqrt{s}=$ 161 GeV, between 110 and 210 GeV at $\sqrt{s}=$ 172 GeV and between 120 and 220 GeV at $\sqrt{s}=$ 183 GeV.

3. The charged particles and calorimeter clusters are grouped into four jets using the Durham algorithm [24]. The jet resolution parameter, y_{34}, at which the number of jets changes from three to four, is required to be larger than 0.007 at $\sqrt{s} = 133$ GeV, and larger than 0.005 at $\sqrt{s} =$161–183 GeV. To discriminate against poorly reconstructed events, a kinematic fit imposing energy and momentum conservation is required to yield a χ^2 probability larger than 0.01. Each of the four jets is required to contain at least two tracks at 133 GeV and at least one track at higher energies. These kinematically constrained jets are used in the subsequent calculation of dijet masses.

4. In the case of the 161–183 GeV data, the background from $e^+e^- \to Z^0\gamma$ is further reduced by eliminating those events where one of the four jets has properties compatible with those of a radiative photon, namely that it has exactly one electromagnetic cluster, not more than two tracks (possibly from a photon conversion), and energy between 45 and 65 GeV at $\sqrt{s}=$ 161 GeV, between 52 and 72 GeV at $\sqrt{s}=$ 172 GeV and between 60 and 80 GeV at $\sqrt{s}=$ 183 GeV.

5. The polar angle of the thrust axis, θ_{thr}, is required to satisfy $|\cos\theta_{\text{thr}}| < 0.9$ at 133 GeV and $|\cos\theta_{\text{thr}}| < 0.8$ at 161–183 GeV.

6. To reduce background from $q\bar{q}$ events, the event shape parameter C [27], which ranges between 0 and 1 and is 0 for a perfect 2-jet event, is required to be larger than 0.7 at $\sqrt{s} =$133 GeV and larger than 0.6 at higher energies.

7. To ensure well-separated jets for better kinematic fits, the angle between any two jets is required to exceed 0.8 radians for 161–183 GeV data.

8. Above the W^+W^- threshold, explicit vetoes against the process $e^+e^- \to W^+W^-$ are applied.

   At $\sqrt{s} =$161 GeV, the two $W^\pm$ bosons are produced with only a small boost. The two jets having the largest opening angle are assigned to one of the $W^\pm$ bosons and the two remaining jets to the other. An event is rejected if both jet pairs have an invariant mass between 75 GeV and 90 GeV.

   At $\sqrt{s} =$172 and 183 GeV, a more sophisticated veto is applied. The four jets are combined into pairs, and for all three combinations the event is refitted constraining the total energy to $\sqrt{s}$ and the total momentum to zero, and also constraining the masses of the two jet pairs to be equal (five constraints). From the three combinations, the one yielding the largest χ^2 fit probability is considered. If the jet pair mass from the fit exceeds 75 GeV and the fit probability is at least 0.01, the event is rejected.

9. To achieve good sensitivity for all ΔM less than 30 GeV, we use two separate mass selections, one relevant for unequal masses and one for equal masses. In both selections, when searching for a signal with a hypothetical sum of masses, M_0, the range $M_0 \pm 2\sigma_M$ is used, where σ_M is 2.0 GeV at $\sqrt{s} =$133 GeV and 3.0 GeV for higher energies. For unequal masses ($\Delta M > 5$ GeV), the event is selected if either the jet association with

the smallest mass difference or the one with the second smallest mass difference has a mass sum M in the range $M_0 \pm 2\sigma_M$. For nearly equal masses ($\Delta M < 5$ GeV), better sensitivity is obtained when considering only the jet association with the smallest mass difference. The resolution σ_M varies only slowly with M and ΔM.

Table 4 presents the number of observed events and the Standard Model expectations before and after the W^+W^- veto (cut 8). The numbers of observed events are consistent with the Standard Model expectations at all centre-of-mass energies both before and after the mass selection.

Data Sample	Without W-Pair Veto		With W-Pair Veto		After Mass Selection	
	Observed	Expected	Observed	Expected	Observed	Expected
133 GeV	18	17.0 ± 0.6	18	17.0 ± 0.6	4	3.1 ± 0.3
161 GeV	11	15.8 ± 0.3	8	13.6 ± 0.3	2	2.7 ± 0.1
172 GeV	36	33.8 ± 0.3	21	16.2 ± 0.2	4	2.9 ± 0.1
183 GeV	190	210.1 ± 1.2	70	81.6 ± 0.8	6	8.9 ± 0.3
Total	255	276.7 ± 1.4	117	128.4 ± 1.1	16	17.6 ± 0.4

Table 4: *Number of observed and expected Standard Model background events before and after the W-pair veto and after adding the mass selection (cut 9) centred at 105 GeV for the smallest ΔM combination. The quoted errors are statistical. No W-Pair veto has been applied to the 133 GeV data.*

Table 5 shows the signal efficiencies for various combinations of (M_X,M_Y) together with the predicted background and the numbers of observed events after all cuts.

Figure 4 shows the distributions of M for the jet associations with the smallest ΔM, and for the jet association with the smallest and second-smallest ΔM, summed over all centre-of-mass energies. Globally, the distributions show consistency between the data and the Standard Model background prediction. In particular, there is no excess in the vicinity of $M \approx 105$ GeV. The overlap of the OPAL-specific analysis and the OPAL emulation of the ALEPH selection has been evaluated in a typical Monte Carlo four-jet signal sample at $\sqrt{s} = 133$ GeV with $M_{h^0} = M_{A^0} = 55$ GeV. In this sample, 59% of the events selected by the OPAL emulation of the ALEPH analysis are also selected by the OPAL-specific analysis.

4.3 Systematic Errors

At $\sqrt{s} = 133$ GeV, since the efficiencies and expected backgrounds for the OPAL emulation of the ALEPH signal are similar to those obtained by ALEPH [1], it is not necessary to consider systematic effects in detail if only numbers of observed events are compared. However, to calculate limits on cross-sections, systematic errors on efficiencies and backgrounds are estimated.

To emulate the ALEPH analysis, the charged multiplicity requirement (cut 9, Section 4.1) on all combinations of two jets was necessary. Since the aim of the emulation analysis is to compare directly the OPAL result with the ALEPH observation, and ALEPH's cross-section

estimate was made assuming a model of four b-jets, we also assume this model. Varying the mean charged multiplicity in b-hadron decays by its measurement uncertainty [28] results in an estimated systematic error of 12% on signal detection efficiencies due to this effect. Including additional uncertainties in the modelling of the cut variables, energy scales, mass resolutions and limited Monte Carlo statistics results in an estimated total systematic error of 13%.

(M_X, M_Y) (GeV)	133 GeV			161 GeV		
	Effic. (%)	Backgd.	Data	Effic. (%)	Backgd.	Data
(50,50)	30.6 ± 1.5	3.2 ± 0.3	3	38.0 ± 2.2	2.4 ± 0.1	3
(40,60)	29.6 ± 2.0	5.6 ± 0.4	6	35.8 ± 2.1	4.2 ± 0.2	3
(55,55)	29.0 ± 2.0	3.1 ± 0.3	4	37.4 ± 1.0	3.0 ± 0.1	1
(50,60)	38.4 ± 1.5	5.6 ± 0.4	7	42.0 ± 2.2	5.0 ± 0.2	1
(40,70)	23.0 ± 1.9	5.6 ± 0.4	7	34.8 ± 2.1	5.0 ± 0.2	1
(60,60)	26.2 ± 1.4	3.2 ± 0.3	3	39.0 ± 2.2	2.8 ± 0.1	0
(50,70)	30.2 ± 2.1	5.6 ± 0.4	4	41.2 ± 2.2	4.8 ± 0.2	1
(60,70)	24.2 ± 1.9	2.2 ± 0.2	4	34.2 ± 2.1	4.7 ± 0.2	2
(50,80)	13.1 ± 1.1	2.2 ± 0.2	4	32.8 ± 2.1	4.7 ± 0.2	2
(70,70)	—	—	—	26.6 ± 2.0	2.0 ± 0.1	2
(60,80)	—	—	—	33.8 ± 2.1	4.4 ± 0.2	3

(M_X, M_Y) (GeV)	172 GeV			183 GeV		
	Effic. (%)	Backgd.	Data	Effic. (%)	Backgd.	Data
(50,50)	31.0 ± 1.5	2.5 ± 0.1	4	19.4 ± 1.8	4.8 ± 0.2	4
(40,60)	24.6 ± 1.9	3.2 ± 0.1	5	16.3 ± 1.6	5.6 ± 0.2	6
(55,55)	34.4 ± 1.0	3.6 ± 0.2	5	31.6 ± 2.1	12.4 ± 0.3	9
(50,60)	32.6 ± 1.5	5.1 ± 0.2	6	22.2 ± 1.9	16.2 ± 0.3	12
(40,70)	23.0 ± 1.3	5.1 ± 0.2	6	18.0 ± 1.7	16.2 ± 0.3	12
(60,60)	33.0 ± 1.5	3.7 ± 0.2	9	32.6 ± 2.1	17.1 ± 0.4	20
(50,70)	34.4 ± 2.1	5.5 ± 0.2	11	23.9 ± 1.9	23.5 ± 0.4	30
(60,70)	33.6 ± 1.5	5.5 ± 0.2	6	32.2 ± 2.1	28.2 ± 0.4	24
(50,80)	28.8 ± 1.4	5.5 ± 0.2	6	23.2 ± 1.9	28.2 ± 0.4	24
(70,70)	29.9 ± 1.4	3.3 ± 0.1	1	31.2 ± 2.1	20.7 ± 0.4	20
(60,80)	31.0 ± 2.1	6.0 ± 0.2	4	27.7 ± 2.0	32.3 ± 0.5	28

Table 5: *Signal detection efficiencies, numbers of expected background events and number of observed data events, for various mass combinations in the OPAL-specific analysis, after the mass selection, cut 9 of section 4.2. The quoted errors are statistical.*

In the OPAL-specific analysis, the signal detection efficiencies are subject to a systematic error of 9%, which includes an allowance for the final state to contain any composition of quark flavours and uncertainties in modelling heavy hadron decays, the uncertainty on the simulation of the decay with regards to fragmentation and hadronization, the modelling of the cut variables, and the limited Monte Carlo statistics.

13

The total relative uncertainty on the residual background is 20% for the OPAL emulation of the ALEPH analysis, and 13% for the OPAL-specific analysis. These errors include the uncertainty on the modelling of the hadronization process, on the prediction of the four-jet rate, W-pair cross-section, and the modelling of the cut variables. The error due to the limited Monte Carlo statistics is added in quadrature to this uncertainty. The systematic errors on the luminosity measurements range from 0.5% to 1.6%.

5   Cross-Section Upper Limits

In the OPAL emulation of the ALEPH analysis, the number of observed events can be compared directly to the ALEPH observation [1] because both the observed background rate and the estimated efficiency are nearly identical to those obtained by ALEPH. From the number of observed and expected events in the dijet mass sum window of 105 ± 4 GeV at $\sqrt{s} \approx 133$ GeV, we set a 95% confidence level (CL) upper limit of 2.1 events that could be attributed to additional cross-section from new physics when scaled to the integrated luminosity of the 1995 ALEPH result. This can be compared to ALEPH's observation in 1995 of nine events with a Standard Model expectation of 0.8 events. To calculate the probability that the OPAL observation is consistent with the ALEPH observation in the presence of a possible signal, the product is formed of the Poisson probability p_1 that at least nine events were observed in ALEPH and p_2 that no more than one event was observed in OPAL, given the Standard Model backgrounds and assuming the presence of a signal scaled by the integrated luminosity. The probability of an outcome no more likely than that observed in the data, i.e., the sum of Poisson probabilities of possible outcomes less than or equal to p_1p_2, is found to be 2.6×10^{-4}, where the hypothesized signal cross-section has been chosen to maximize this probability.

Assuming production of new particles X and Y subsequently decaying to a final state of four b-jets to determine efficiencies, cross-section upper limits are set using the OPAL emulation of the ALEPH analysis. From the number of observed and expected events in the dijet mass sum window as above at $\sqrt{s} \approx 133$ GeV, a 95% confidence level (CL) upper limit of 1.4 pb is determined for the production cross-section at the dijet mass sum of 105 GeV. Systematic uncertainties of efficiency, background and luminosity are taken into account using the procedure outlined in Reference [29].

To combine data from different centre-of-mass energies, we consider two different functions for the energy dependence of the cross-section of a hypothetical signal. It is first assumed that the cross-section varies as $\beta(3 - \beta^2)/s$, typical for pair-production of spin-1/2 particles, where β is taken as the average velocity of the particles in the laboratory frame [30]. Taking from Table 3 the total number of observed and expected events in resolution-dependent mass windows around 105 GeV, an upper limit on the production cross-section at 133 GeV of 0.58 pb at 95% CL is found. Secondly, under the hypothesis that the signal cross-section varies as β^3/s, typical for the production of scalar particles [30], the upper limit on the cross-section at 133 GeV is computed to be 0.31 pb at 95% CL. These limits can be compared to ALEPH's estimated cross-section of 3.1 ± 1.7 pb [1] from their total number of excess events.

The OPAL-specific analysis described in section 4.2 is used to obtain upper limits for the cross-section of a possible signal process $e^+e^-\to XY\to$ four jets, in the presence of background from Standard Model processes, using Poisson statistics and incorporating systematic uncertainties as described in Reference [29]. The process $e^+e^-\to h^0A^0$ was used to model the signal detection efficiencies. The resulting 95% CL upper limits, as function of the mass sum $M(\equiv M_X + M_Y)$, are shown in Figure 5, for ΔM close to zero and $\Delta M = 30$ GeV. A mass window of $M \pm 2\sigma_M$ is scanned across the distribution of the dijet mass sum in small steps. To account for a possible discrepancy between the mass scale of the data and the Monte Carlo in a conservative manner, the mass window is displaced by ± 0.5 GeV at each scan point. The largest data count in any of the three windows including the nominal one and the smallest background estimation in any of the three windows are used to compute the limit. When results at different centre-of-mass energies are combined, the hypothetical production cross-section is assumed to vary as β^3/s. The cross-section limits are presented separately for the 133 GeV data, and for all data (130–184 GeV) combined. Limits on the cross-section from the combined data sample are computed both at $\sqrt{s} = 133$ GeV and at $\sqrt{s} = 183$ GeV. These results are independent of the flavour of the quarks from the decay of the hypothesized particles and are valid for X and Y being scalars produced predominantly by an s-channel process.

6 Conclusions

Following the ALEPH observation of a large excess of four-jet events with dijet mass sums around 105 GeV at $\sqrt{s} \approx 133$ GeV [1], a careful emulation of the ALEPH analysis has been performed using OPAL data collected from e^+e^- collisions at centre-of-mass energies between 130 and 184 GeV. The process $e^+e^- \to h^0A^0$ was used to estimate the signal detection efficiencies. The estimated sensitivity, mass resolution, efficiency, and estimated backgrounds in this analysis were similar to that of the ALEPH analysis. No significant excess of four-jet events with dijet mass sums in the region close to 105 GeV, or any other region between 60 and 160 GeV, has been observed in any of the data samples separately or combined, and our observations are consistent with Standard Model predictions. The same conclusions are reached when an OPAL-specific analysis is employed. Limits for the cross-section of a hypothetical process $e^+e^-\to XY\to$ four jets are given as a function of the dijet mass sum M and the mass difference ΔM. The 95% confidence upper limits obtained in both analyses for dijet mass sums near 105 GeV are below the excess reported in 1995 by ALEPH [1] to a high degree of confidence. ALEPH has recently analysed [31] new data at centre-of-mass energies between 130 and 184 GeV and do not confirm the previously reported excess.

Acknowledgements

References

[1] ALEPH Collab., D. Buskulic *et al., Z. Phys.* **C71** (1996) 179.

[2] OPAL Collab., G. Alexander *et al., Z. Phys.* **C73** (1997) 201.

[3] B. Pietrzyk, *The ALEPH Four-Jet Story*, LAPP-EXP-97.02, 5 May 1997, to be published in the proceedings of 33rd Rencontre de Moriond: QCD and High Energy Hadronic Interactions, Les Arcs, France, 22–29 March 1997.

[4] DELPHI Collab., P. Abreu *et al., Z. Phys.* **C73** (1996) 1.

[5] L3 Collab., *Search for anomalous four-jet events in e^+e^- annihilation at $\sqrt{s} = 130 - 172$ GeV*, CERN preprint CERN-PPE/97-57, 30 May 1997, to be published in *Phys. Lett. B.*

[6] V. Barger, W.-Y. Keung and R.J.N. Phillips, *Phys. Lett.* **B364** (1995) 27.

[7] D. Choudhury and D.P. Roy, *Phys. Rev.* **D54** (1996) 6797;
P. Chankowski, D. Choudhury and S. Pokorski, *Phys. Lett.* **B389** (1996) 677;
D.K. Ghosh and R.M. Godbole, *Z. Phys.* **C75** (1997) 357;
G.R. Farrar, *Phenomenology of Charginos and Neutralinos in the Light Gaugino Scenario*, preprint RU-96-71, e-Print Archive: hep-ph/9608387;
G.R. Farrar, *Phys. Rev. Lett.* **76** (1996) 4115;
A.K. Grant, R.D. Peccei, T. Veletto and K. Wang, *Phys. Lett.* **B379** (1996) 272;
S.F. King, *Phys. Lett.* **B381** (1996) 291;
H. Dreiner, S. Lola and P. Morawitz, *Phys. Lett.* **B389** (1996) 62.

[8] N.D. Hari Dass and V. Soni, *An Asymptotically Free Extension of QCD and ALEPH Four-jet Events*, preprint hep-ph/9709391;
M. Carena, G.F. Giudice, S. Lola and C.E.M. Wagner, *Phys. Lett.* **B395** (1997) 225.

[9] ALEPH Collab., D. Buskulic *et al., Search for charged Higgs bosons in e^+e^- collisions at centre-of-mass energies from 130 to 172 GeV*, CERN-PPE/97-129, submitted to *Phys. Lett. B.*

[10] OPAL Collab., K. Ahmet *et al., Nucl. Inst. Meth.* **A305** (1991) 275.

[11] P.P. Allport *et al., Nucl. Inst. Meth.* **A346** (1994) 476;
S. Anderson *et al., The Extended OPAL Silicon Strip Microvertex Detector*, CERN-PPE/97-092, to be published in *Nucl. Instr. Meth.*

[12] B.E. Anderson *et al., IEEE Transactions on Nuclear Science* **41** (1994) 845.

[13] OPAL Collab., K. Ackerstaff *et al., Tests of the Standard Model and Constraints on New Physics from Measurements of Fermion-pair Production at 130–172 GeV at LEP*, CERN-PPE/97-101, to be published in *Eur. Phys. J. C.*

[14] The LEP Energy Working Group, *LEP Energy Calibration in 1996*, LEP Energy Group/97-01, March 1997; *Energies for LEP1.5 run*, LEP Energy Group/97-04, July 1997; `http://www.cern.ch/LEPECAL/reports/reports.html` (for 1995–1996 centre-of-mass

energies); P. Wells and LEP Energy Working Group, personal communication (preliminary for 1997 centre-of-mass energies).

[15] PYTHIA 5.721 and JETSET 7.408 generators: T. Sjöstrand, Comp. Phys. Comm. **82** (1994) 74; T. Sjöstrand, LUTP 95-20.

[16] EXCALIBUR generator: F.A. Berends, R. Pittau, R. Kleiss, Comp. Phys. **85** (1995) 437.

[17] J. Fujimoto *et al.,* Comp. Phys. Comm. **100** (1997) 128.

[18] HERWIG generator: G. Marchesini *et al.,* Comp. Phys. Comm. **67** (1992) 465.

[19] R. Engel and J. Ranft *Phys. Rev.* **D54** (1996) 4244.

[20] HZHA generator: P. Janot, in Physics at LEP2, edited by G. Altarelli, T. Sjöstrand and F. Zwirner, CERN 96-01, Vol. 2, p. 309.

[21] J. Allison *et al., Nucl. Inst. Meth.* **A317** (1992) 47.

[22] OPAL Collab., G. Alexander *et al., Z. Phys.* **C52** (1991) 175.

[23] OPAL Collab, K. Ackerstaff *et al., Phys. Lett.* **B389** (1996) 616.

[24] N. Brown and W.J. Stirling, *Phys. Lett.* **B252** (1990) 657;
S. Bethke, Z. Kunszt, D. Soper and W.J. Stirling, *Nucl. Phys.* **B370** (1992) 310;
S. Catani *et al., Phys. Lett.* **B269** (1991) 432;
N. Brown and W.J. Stirling, *Z. Phys.* **C53** (1992) 629.

[25] Particle Data Group, *Phys. Rev.* **D50** (1994) 1281.

[26] OPAL Collab., G. Alexander *et al., Phys. Lett.* **B376** (1996) 232.

[27] G. Parisi, *Phys. Lett.* **B74** (1978) 65;
J.F. Donoghue, F.E. Low and S.Y. Pi, *Phys. Rev.* **D20** (1979) 2759.

[28] OPAL Collab., R. Akers *et al., Z. Phys.* **C61** (1994) 209; DELPHI Collab., P. Abreu *et al., Phys. Lett.* **B347** (1995) 447. The weighted average allows for a variation of ± 0.35 in the mean charged multiplicity of b hadrons.

[29] R.D. Cousins and V.L. Highland, *Nucl. Inst. Meth.* **A320** (1992) 331.

[30] See for example V.D. Barger and R.J.N. Phillips, *Collider Physics*, Frontiers in Physics Lecture Note Series, Addison-Wesley (1987) p. 120.

[31] ALEPH Collab., D. Buskulic *et al., Four-jet final state production in e^+e^- collisions at centre-of-mass energies ranging from 130 to 184 GeV*, CERN-PPE/97-156, submitted to *Phys. Lett. B.*

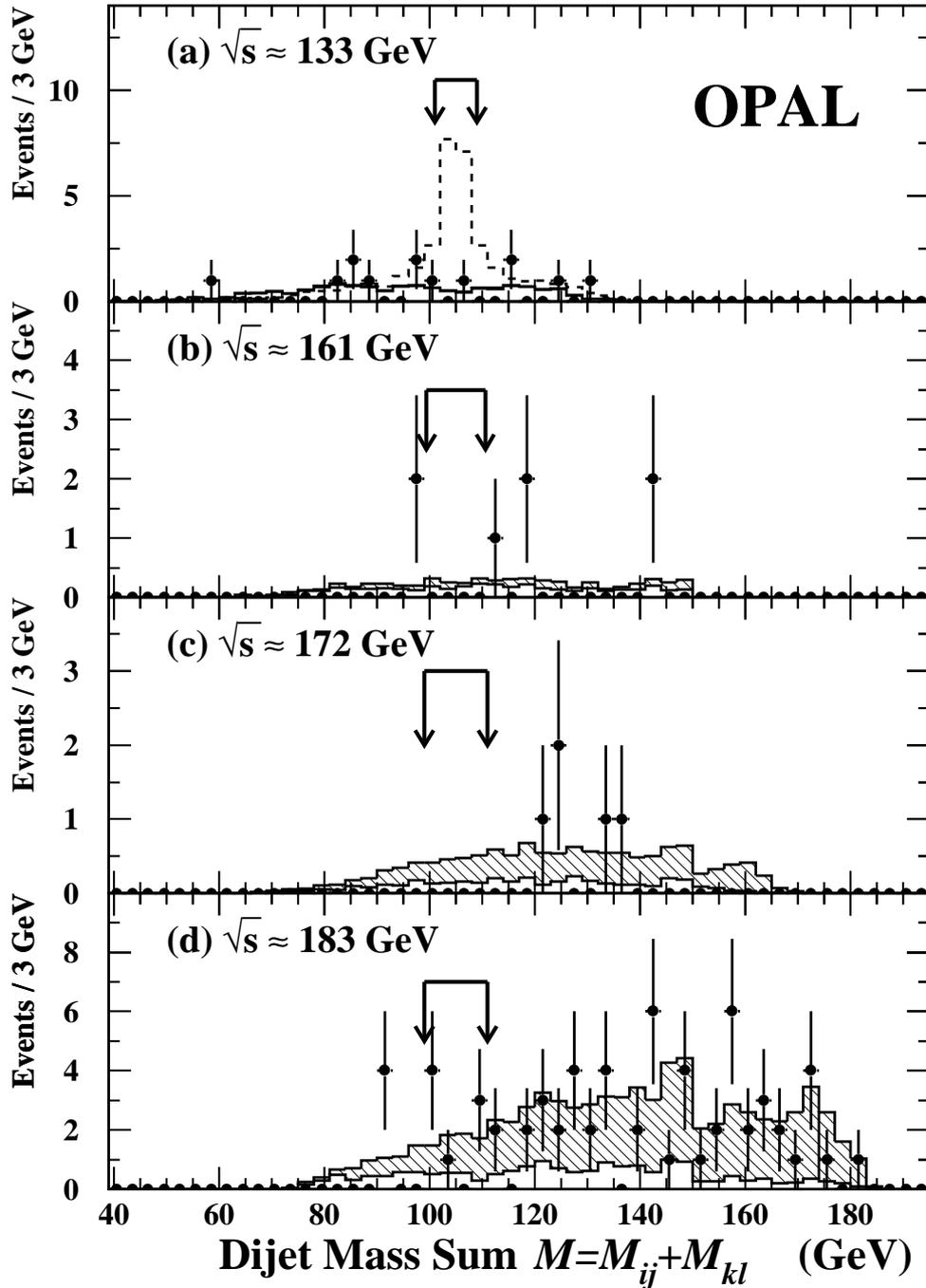Figure 1: *The dijet mass sum for the combination with the smallest ΔM after the W-pair veto in OPAL's emulation of the ALEPH analysis shown separately for the different centre-of-mass energies. Data are shown by the points and Standard Model backgrounds by the histograms. The hatched component of the background histograms denotes Standard Model four-fermion processes, while the unhatched component denotes $Z^0/\gamma^* \to q\bar{q}$. The mass windows containing the region of interest are indicated by the arrows. The dashed histogram in (a) illustrates a signal (plus background) that could be expected due to $h^0 A^0$ with both decaying to pairs of b-quark jets, and $M_{h^0} = M_{A^0} = 52.5$ GeV, normalized to the excess observed by ALEPH at $E_{cm} \approx 133$ GeV [1].*
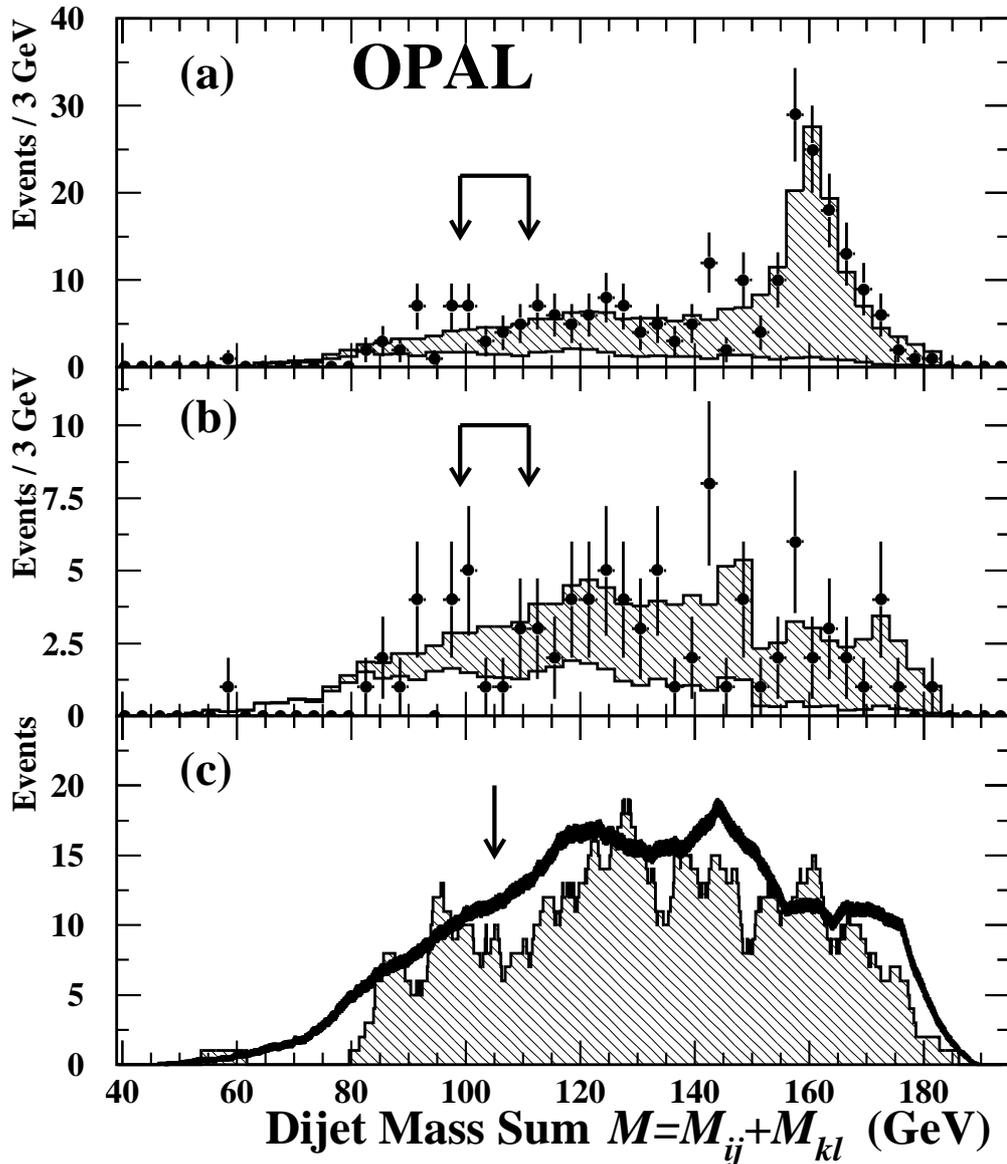
Figure 2: *The dijet mass sum in OPAL's emulation of the ALEPH analysis for the combined 130–184 GeV samples. Plots (a) and (b) show the distribution of the dijet mass sum before and after the W-pair veto, respectively. Data are shown by the points and Standard Model backgrounds by the histograms. The hatched component of the background histograms denotes Standard Model four-fermion processes and the unhatched component denotes $Z^0/\gamma^* \to q\bar{q}$. The mass window around 105 GeV whose width accommodates the resolution at $\sqrt{s} = 183$ GeV, is shown with the arrows. Plot (c) shows the sliding mass window scan for the same analysis after the W-pair veto. The hatched histograms show the total number of data events, and the solid line shows the Standard Model expectation; the line width indicates the Monte Carlo statistical error. An arrow is drawn at 105 GeV.*
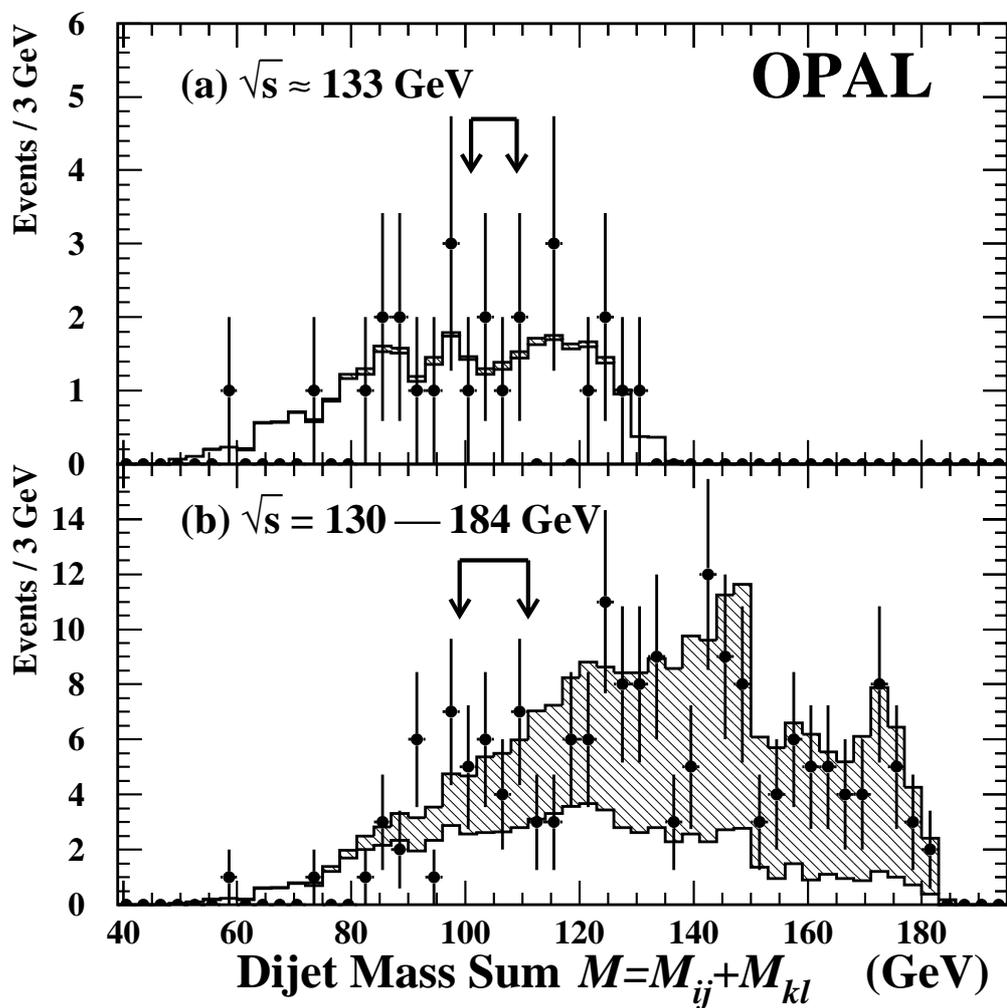
20

Figure 3: *The dijet mass sum in OPAL's emulation of the ALEPH analysis for both the combination with the smallest ΔM and the combination with the second-smallest ΔM for (a) the 133 GeV data sample and (b) the combined 130–184 GeV samples. The points and histograms are as in Figure 1.*
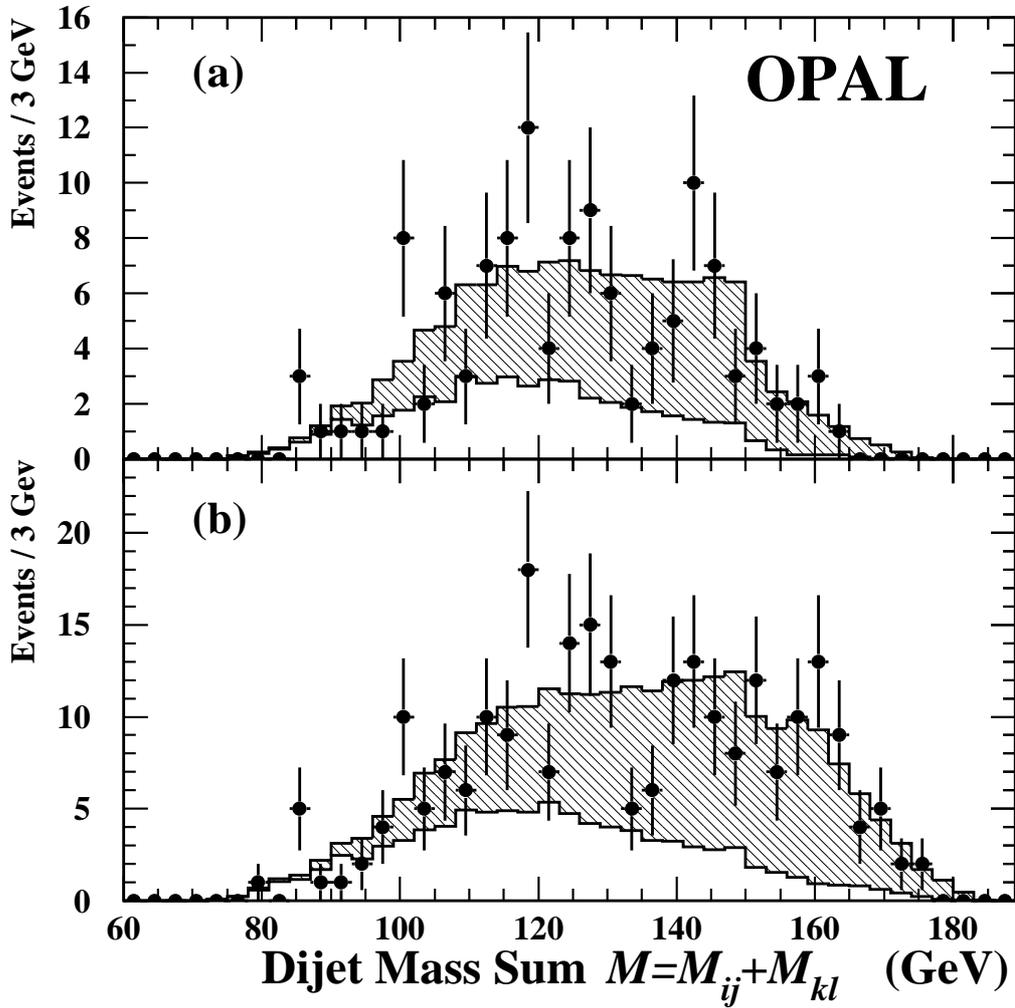
Figure 4: *Distributions of M in the OPAL-specific analysis for the combined 130–184 GeV samples after all selection requirements except the mass selection (cut 9), (a) for the jet combination with the smallest ΔM and (b) for the jet combinations with the smallest and second-smallest ΔM. The points and histograms are as in Figure 1.*
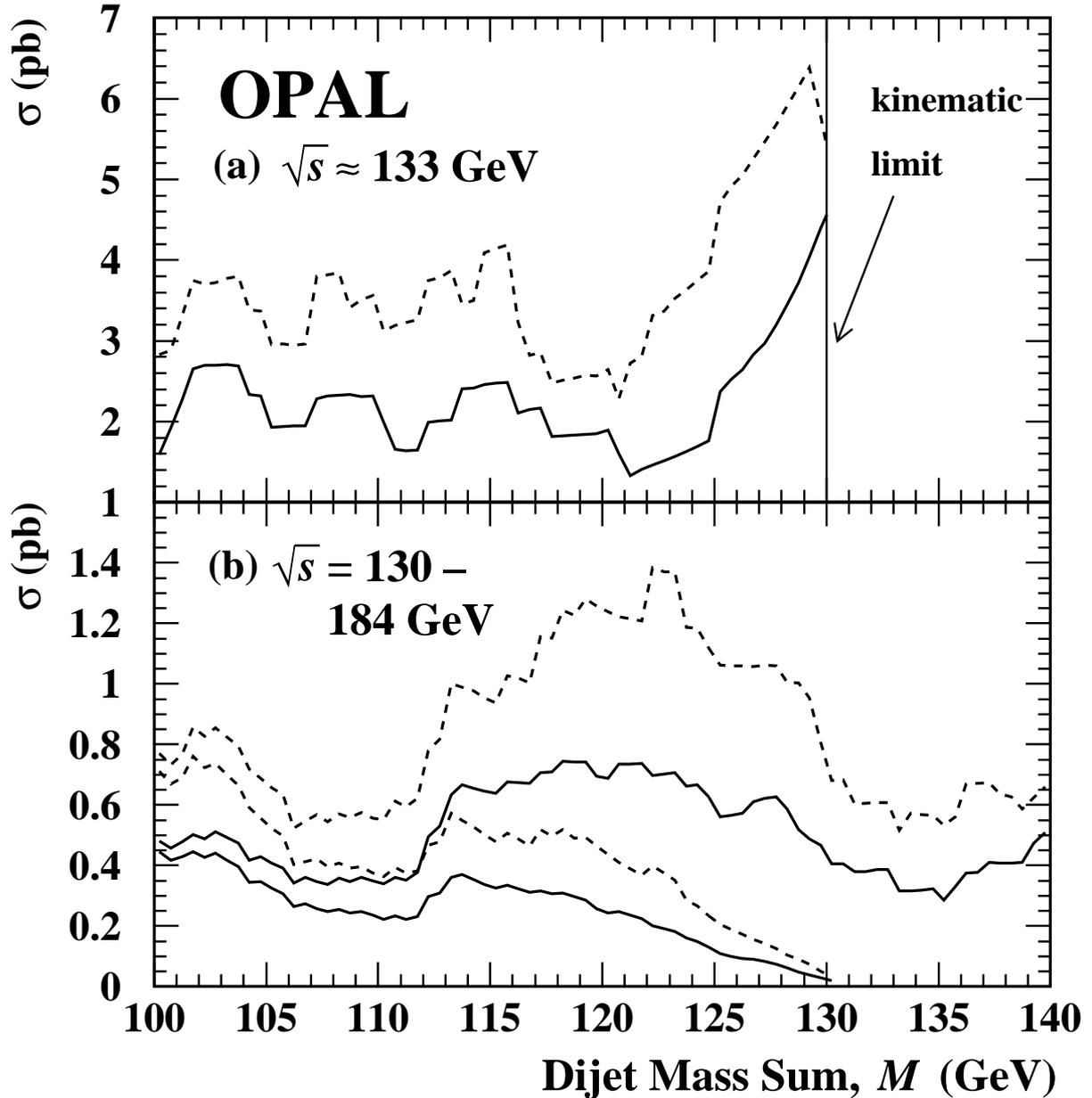
Figure 5: *The 95% CL upper limits obtained with the OPAL-specific analysis on the production cross-section of a possible signal as a function of M for* ΔM *close to 0 (solid lines) and for* ΔM < 30 *GeV (dashed lines). Plot (a) shows the limits computed using the data collected at* $\sqrt{s} \approx 133$ *GeV; plot (b) shows the limits using the combined data from* $\sqrt{s} = 130\text{--}184$ *GeV assuming a cross-section that varies as* β^3/s *scaled to* $\sqrt{s} = 133$ *GeV (lines that end near M=130 GeV) and* $\sqrt{s} = 183$ *GeV (lines that extend to larger M).*